

HIGH-INTENSITY BEAM OPERATIONS IN THE J-PARC 3-GeV RCS

H. Hotchi*, H. Harada, P.K. Saha, Y. Shobuda, F. Tamura, K. Yamamoto, M. Yamamoto,
Japan Atomic Energy Agency (JAEA), Tokai, Naka, Ibaraki, 319-1195 Japan
Y. Irie,

High Energy Accelerator Research Organization (KEK), Tsukuba, Ibaraki, 305-0801 Japan

Abstract

Since December 2009, we have started a beam tuning for high-intensity beams including the beam painting injection scheme. By optimizing the beam painting parameters, we successfully demonstrated a 300-kW beam operation at $\sim 1\%$ intensity loss. In this paper, we present recent progress in the course of our beam power ramp-up scenario together with the corresponding space-charge simulations.

INTRODUCTION

The J-PARC accelerator complex [1] consists of a 400-MeV linac, a 3-GeV rapid cycling synchrotron (RCS), a 50-GeV main ring synchrotron (MR) and several experimental facilities (a materials and life science experimental facility; MLF, a hadron experimental hall, and a neutrino beam line to Kamioka), in which the RCS has two functions as a proton driver to the MLF and as an injector to the MR. A negative hydrogen ion (H^-) beam from the linac is delivered to the RCS injection point, where it is multi-turn charge-exchange injected with a carbon stripper foil. The RCS accelerates the injected beam up to 3 GeV at 25 Hz repetition. With the current injection energy of 181 MeV, the RCS aims at providing 300 kW output beam power. After upgrading the linac energy to 400 MeV by adding an annular coupled structure (ACS) linac, the RCS will aim at 1 MW output.

The J-PARC beam commissioning started in November 2006 and it has well proceeded as planned from the linac to the downstream facilities. The RCS was beam commissioned in October 2007 and then started the user operation with 4~20 kW output beam power in December 2008. Via the underlying beam studies with such a low intensity beam, the output beam power from the RCS has been increased to 120 kW since December 2009. Since then, our effort has been focused on a parameter tuning for higher-intensity beams (300 kW~) including the beam painting injection scheme.

One of key issues to achieve such a high intensity operation is to decrease and localize beam losses. In high intensity proton machines like the RCS, the space-charge effect will make a severe limitation on the achievable beam intensity. In order to mitigate the space-charge effect, the RCS adopts a multi-turn painting injection scheme in both the transverse and longitudinal phase spaces. The permissible range of intensity loss for 300 kW output operation with 181 MeV injection energy, which is determined by

the current collimator capability of 4 kW, is 22% at the injection energy. On the other hand, the allowable intensity loss for 1 MW output operation with 400 MeV injection energy is 3% if assuming the same collimator limit at the injection energy. The above two operations give an equivalent space-charge effect at each injection energy. Therefore, achieving 300 kW output with less than 3% intensity loss for 181 MeV injection energy is the first matter to realize 1 MW output with 400 MeV injection energy.

BEAM LOSS REDUCTION BY THE PAINTING INJECTION

Via a series of basic beam tuning measurement and the underlying beam studies mainly related to single-particle behavior [2], we began on a parameter tuning for higher intensity beams including the beam painting injection scheme.

Fig. 1 shows beam survival rates measured with a DC current transformer (DCCT) for different intensities and painting parameters (1)~(9) listed in Table 1. The intensity losses observed for (1)~(5) with no painting were 0.5~7% depending on the beam intensity only appearing around the injection energy. For 300 kW-equivalent intensity beams causing $\sim 7\%$ intensity loss, we performed the painting injection aiming at the beam loss reduction. As for the transverse painting [3], 100π mm mrad correlated painting was performed by sweeping the closed orbit in the horizontal plane and the injection orbit in the vertical plane. On the other hand, the longitudinal painting [4] was performed by combination of the momentum-offset injection scheme, where the rf frequency had an offset (0~−0.2% in momentum), and superposing a second harmonic rf voltage with an amplitude of 80% of the fundamental one. The phase sweep of the second harmonic rf voltage relative to the fundamental one (−80 to 0 degrees) was also employed. As shown in (6) and (9) of Fig. 1, the intensity loss was improved to $\sim 5\%$ by the transverse painting, and finally minimized to $\sim 1\%$ by adding the longitudinal painting. In the figure, the blue dotted curves and blue circles are the results from the corresponding space-charge simulations using a fully 3D particle-in-cell code called SIMPSONS [5] including the following lattice imperfections; (A) scattering on the charge-exchange foil, (B) static leakage fields from the extraction beam line, (C) field and alignment errors, (D) edge focus of the injection-orbit bump magnets, and (E) multipole field components for all the ring magnets, where (B)~(E) are based on measurements. The calculated ones almost well reproduced the measured intensity losses

* hotchi.hideaki@jaea.go.jp

Table 1: Experimental conditions, where $I_{peak}/L_{macro}/\text{Chop}$ show peak current/macro-pulse length/chopper beam-on duty factor of the injection beam, N_{bunch}/N_{part} are bunch number/particles per pulse, ϵ_{tp} is the transverse painting emittance, and $V_{2nd}/\Delta\phi/\Delta p$ show amplitude of 2nd harmonic rf voltage (ratio to the fundamental one)/phase sweep of 2nd harmonic rf voltage relative to the fundamental one/momentum offset applied in the longitudinal painting.

Data ID	I_{peak} (mA)	L_{macro} (ms)	Chop (%)	N_{bunch}	N_{part}	Intensity (kW)	ϵ_{tp} (π mm mrad)	V_{2nd} (%)	$\Delta\phi$ (deg)	Δp (%)
(1)	15	0.1	56	2	5.0×10^{12}	60	-	-	-	-
(2)	15	0.2	56	2	1.0×10^{13}	120	-	-	-	-
(3)	15	0.3	56	2	1.5×10^{13}	180	-	-	-	-
(4)	15	0.4	56	2	2.0×10^{13}	240	-	-	-	-
(5)	15	0.5	56	2	2.5×10^{13}	300	-	-	-	-
(6)	15	0.5	56	2	2.5×10^{13}	300	100	-	-	-
(7)	15	0.5	56	2	2.5×10^{13}	300	100	80	-80	-
(8)	15	0.5	56	2	2.5×10^{13}	300	100	80	-80	-0.1
(9)	15	0.5	56	2	2.5×10^{13}	300	100	80	-80	-0.2

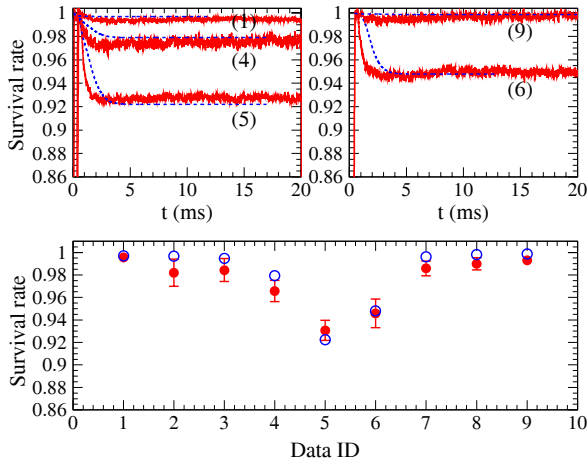


Figure 1: Beam survival rates measured with DCCT for different intensities and painting parameters listed in Table 1, where the blue dotted curves and blue circles are the results from the corresponding space-charge simulations. The quoted errors in the lower figure are pulse-by-pulse deviations in rms.

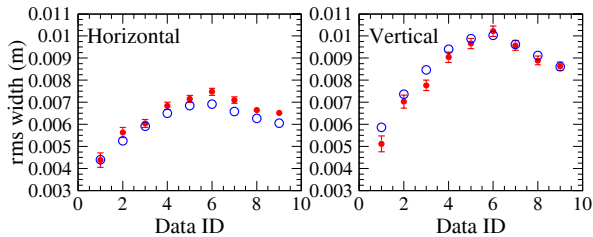


Figure 2: Transverse profile widths (rms) at 3 GeV measured with a multi-wire profile monitor located at the extraction beam line, where the blue circles are the calculated ones.

for different intensities and painting parameters. As shown in Fig. 2 and 3, the calculated transverse profiles at 3 GeV and bunching factors for the first 2 ms are also in good agreement with the measured ones. These results support that our simulation adequately catch the behavior of the actual beams.

04 Hadron Accelerators

A15 High Intensity Accelerators

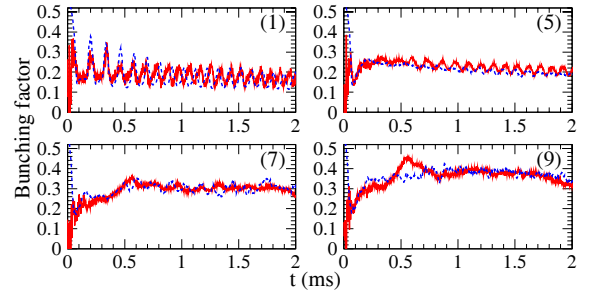


Figure 3: Bunching factors for the first 2 ms measured with a wall current monitor, where the dotted blue curves are the calculated ones.

Fig. 4 shows incoherent tune spreads for the cases of (5) and (9) calculated at the end of the injection period. The current painting mitigates the space-charge detuning from ~ -0.6 to ~ -0.4 . In order to understand the mechanism of the beam loss reduction by the current painting, we checked a time dependence of the beam moments obtained from the simulated transverse particle distributions. The influence of the resonance to the particle motion is reflected in the coherent oscillation of the corresponding beam moment; if the beam is captured in a resonance, the tune of the corresponding beam moment gets to integer. Fig. 5 shows FFT spectra of the 2nd, 3rd, and 4th-order coherent oscillations calculated for (5) and (9). While the spectra for $\langle x^2 \rangle$, $\langle y^2 \rangle$, $\langle x^3 \rangle$, $\langle x^4 \rangle$, $\langle x^2 y^2 \rangle$ and $\langle y^4 \rangle$ have a significant peak at integer, they are significantly mitigated by the current painting. From this analysis, we could say that the beam losses observed with no painting are mainly from the particles which satisfy the even-order parametric resonance conditions for $Q=6$. Fig. 6 shows normalized 99.9% emittances for (5) and (9) calculated with the systematic combinations of the lattice imperfections (A)~(E), where the ring collimator aperture is not set to see the emittance growth in more detail. As shown in the figure, the emittance growth at the early stage of acceleration is significantly reduced by the painting. In performing the painting, the events surpassing the collimator aperture is mainly from the emittance dilution caused by the foil scattering.

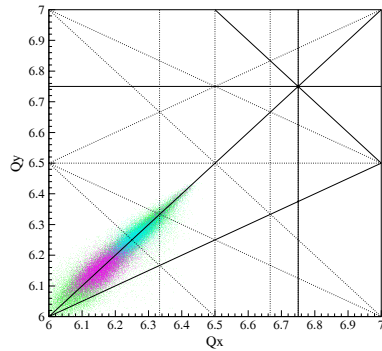


Figure 4: Incoherent tune shifts calculated at the end of the injection, where the green and pink ones are for (5) and (9), and the light blue one is that calculated with the design painting parameters; the combination of the 200π mm mrad transverse painting and longitudinal painting applied for (9).

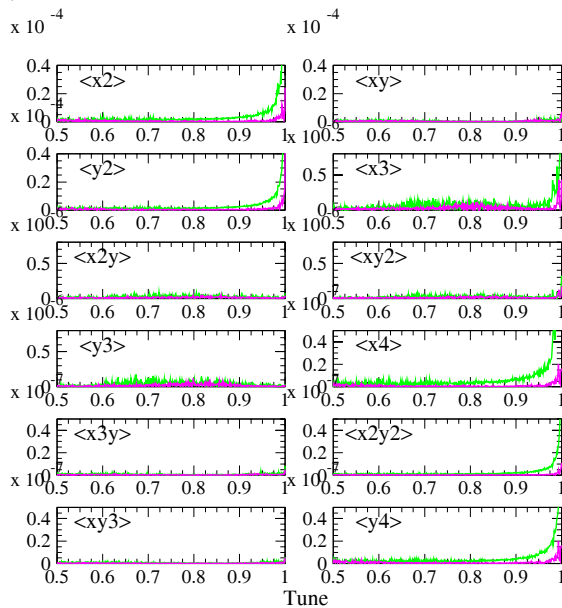


Figure 5: FFT spectra of the 2nd, 3rd and 4th-order coherent oscillations, where the green ones are calculated for (5), and the pink ones are for (9).

ISSUES AND FUTURE PROSPECT

The intensity losses for 300 kW-equivalent intensity beams were minimized to a low level of 1% by the painting and it was experimentally confirmed that most of them were well localized at the ring collimator section [6]. In order to minimize the foil scattering loss [7] which makes ~ 1.5 mSv/h residual radiations in the current user operation with 120 kW output beam power, we will introduce the new foil with a size optimized for the injection beam width in this summer maintenance period. After completing such an improvement, we plan to try long-term continuous operations first with 200 kW output and then step to 300 kW output beam power.

In aiming at providing higher intensity beams, it is essential to perform finer beam tuning considering the quality of the extraction beams as well as the reduction of the

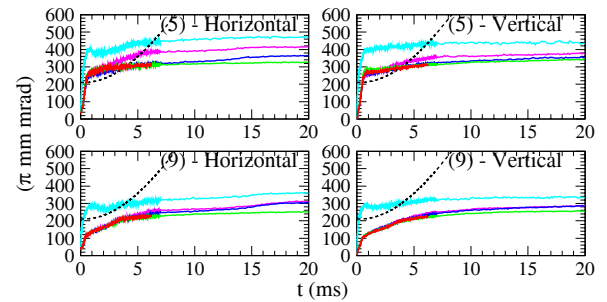


Figure 6: Normalized 99.9% emittances for (5) and (9) calculated with the systematic combinations of the lattice imperfections; the light blue ones with all (A)~(E), the pink ones with (B)~(E), the blue ones with (C)~(E), the green ones with (D)~(E) and the red ones with only (E). While the ring collimator aperture is not set in this calculation, the dotted black curves correspond to the ring collimator aperture of 324π mm mrad.

beam losses. As for the MLF, uniformly shaped beams are required to mitigate the pitting damage on the mercury target, while for the MR, sufficient beam halo reductions are essential because of its narrow physical aperture (54π mm mrad). For such requirements, one of the key knobs is the beam painting. While the longitudinal painting has been successfully carried out as designed, the painting emittance in the transverse plane is still limited to $\sim 100\pi$ mm mrad. The design transverse painting emittance is 216π mm mrad. In introducing such a transverse painting, considerable intensity losses of $\sim 10\%$ take place at the moment, though the space-charge detuning should be significantly mitigated as shown in the light blue scatter plot in Fig. 4. From the simulation studies, it is clarified that such a situation is from the beta beating caused by the edge focus of the injection-orbit bump magnets. Namely the edge focus makes a significant distortion of the lattice periodicity especially in the vertical plane, leading to a shrinkage of the dynamic aperture through various induced non-systematic harmonic components. For this concern, now we discuss the introduction of 2nd harmonic corrector system for the beta beating compensation. It can also be applied to a fast tune control in the acceleration process. Such a system would give us better flexibility for the operating tune as well as the beam painting.

REFERENCES

- [1] JAERI-Tech 2003-044 and KEK Report 2002-13
- [2] H. Hotchi *et al.*, Phys. Rev. ST Accel. Beams **12**, 040402 (2009).
- [3] P.K. Saha *et al.*, Phys. Rev. ST Accel. Beams **12**, 040403 (2009).
- [4] F. Tamura *et al.*, Phys. Rev. ST Accel. Beams **12**, 041001 (2009).
- [5] S. Machida and M. Ikegami, AIP Conf. Proc. 448, p.73, 1998.
- [6] K. Yamamoto *et al.*, in these proceedings.
- [7] H. Harada *et al.*, in these proceedings.